

ACCEPTED MANUSCRIPT • OPEN ACCESS

Design of a programmable particle filtering medium using a novel auxetic metamaterial

To cite this article before publication: Hafiz Muhammad Asad Ali *et al* 2023 *Smart Mater. Struct.* in press <https://doi.org/10.1088/1361-665X/accee9>

Manuscript version: Accepted Manuscript

Accepted Manuscript is “the version of the article accepted for publication including all changes made as a result of the peer review process, and which may also include the addition to the article by IOP Publishing of a header, an article ID, a cover sheet and/or an ‘Accepted Manuscript’ watermark, but excluding any other editing, typesetting or other changes made by IOP Publishing and/or its licensors”

This Accepted Manuscript is © 2023 The Author(s). Published by IOP Publishing Ltd.



As the Version of Record of this article is going to be / has been published on a gold open access basis under a CC BY 4.0 licence, this Accepted Manuscript is available for reuse under a CC BY 4.0 licence immediately.

Everyone is permitted to use all or part of the original content in this article, provided that they adhere to all the terms of the licence <https://creativecommons.org/licenses/by/4.0>

Although reasonable endeavours have been taken to obtain all necessary permissions from third parties to include their copyrighted content within this article, their full citation and copyright line may not be present in this Accepted Manuscript version. Before using any content from this article, please refer to the Version of Record on IOPscience once published for full citation and copyright details, as permissions may be required. All third party content is fully copyright protected and is not published on a gold open access basis under a CC BY licence, unless that is specifically stated in the figure caption in the Version of Record.

View the [article online](#) for updates and enhancements.

Design of a programmable particle filtering medium using a novel auxetic metamaterial

Hafiz M. A. Ali, Meisam Abdi*, S. Abolfazl Zahedi, Yong Sun

School of Engineering and Sustainable Development, De Montfort University, Leicester LE1 9BH, UK

**meisam.abdi@dmu.ac.uk*

Abstract

This manuscript aims to design and develop a 2D auxetic filtering medium with programmable geometric features specifically designed to vary under in-plane tensile strain. This feature empowers the filtering medium to control the particles separation. A novel design and optimisation algorithm developed in Matlab® determines the final optimized geometry of the filtering medium based on the desired particle size input. Upon thorough numerical investigation, an empirical relationship between the linear elastic in-plane tensile strain and aperture size of the proposed metamaterial is revealed. This empirical relation can be used in mechatronic and control systems to steer the proposed filtering medium. A prototype of such filtering medium capable of classification of particles of size 4mm to 4.5mm, when subjected to linear strain, is fabricated through Fused Deposition Modelling (FDM) process. The developed geometry configurations in this research are scalable, providing a potential cost-effective and efficient solution for industrial applications including reconfigurable filtration and segregation systems.

Keywords: *Auxetic, Metamaterial, Additive manufacturing, Particle filter, Programmable, Genetic algorithm, Optimization*

1. Introduction

There has been a growing interest in modern industries in the intelligent design of materials and structures with properties and functionalities that may not be achievable by conventional material design. Mechanical metamaterials are man-made materials, the properties of which depend predominantly on their geometrical construction. This advantage allows designers to acquire tailored physical and mechanical properties. Metamaterials exhibit exceptional properties, and recent advancements in additive manufacturing (AM) have enabled their use in applications that are unachievable with conventional or naturally occurring materials [1]. Metamaterials are made of an elementary geometry called a *unit cell*. A unit cell holds and defines all the characteristics and functionalities of the metamaterial when combined and arranged in a repetitive order in a spatial space. This arrangement of unit cells is called a *lattice structure* [2], [3]. Metamaterial properties primarily depend upon the geometry of the unit cell rather than only relying on the building material from which it is fabricated from [2], [4]. A unique design of a unit cell for a metamaterial allows for achieving unique physical properties like an unfeleability cloak [5], [6] and optical properties like a negative refractive index [7].

Poisson's ratio (ν) is a property of a material that indicates the negative of the ratio of transverse strain to axial strain [8]. It is a unitless number that is commonly positive (usually ranging from 0.25 to 0.5) for naturally occurring materials or '*non-auxetics*' (Figure 1 (a)). Conversely, materials with auxetic properties exhibit a contrary response, whereby they shrink when subjected to compression and expand when pulled by tension, owing to their negative Poisson's ratio (NPR) behaviour (Figure 1 (b)). Auxetic behaviour has also been observed in several natural and biological materials [9]. Similarly, several studies have presented the development of zero Poisson's ratio (ZPR) metamaterials for various

applications, such as shape recovery and energy absorption some researchers designed Zero Poisson's Ratio or ZPR metamaterials which show interesting shape recovery and energy absorption features [10], [11] & [12].

In addition to auxetic behaviour, there are many other artificial mechanical behaviours like negative stiffness, negative compressibility, and ultra-lightweight ultra-high stiffness properties that are achievable through different types of mechanical metamaterials [10], [13]. Such properties are controllable by tuning the unit-cell geometry through several methods like computer-aided design (CAD) and topology optimisation [12], [14], [15].

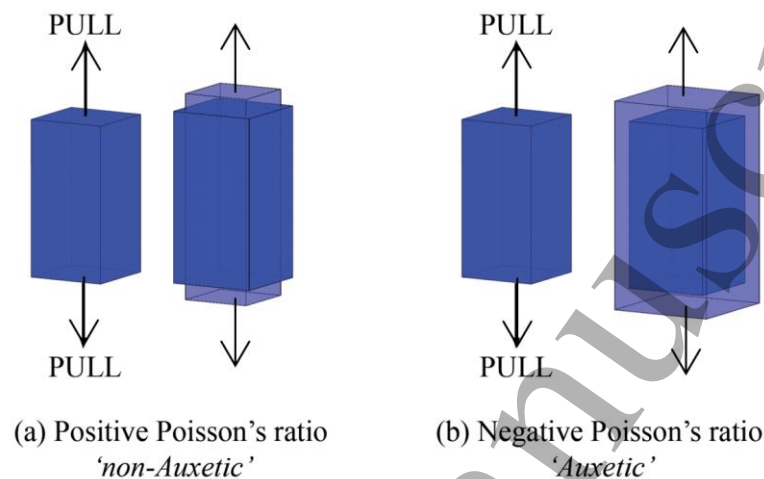


Figure 1 The schematic of material's response under a tensile load; (a) positive Poisson's ratio and (b) negative Poisson's ratio

Due to this unique behaviour, auxetics have been considered for different applications such as prosthetics [16], tissue engineering [17], sports practice [18], textile industry [19], biomechanical [20], vibration isolation [21] and enhanced thermo-mechanical applications [22]. Silva *et al.* [23] presented a comprehensive review on the chemical composition, and physical and mechanical properties of the cork material and signified its products and sub-products. Cork is a naturally occurring material made of suberin polymer microstructure usually used as a glass bottle cap. This material has a ZPR. Therefore, opening and sealing a glass bottle does not produce lateral pressure on the bottleneck due to compressive and tensile forces. This behaviour is essential in order to prevent breaking the glass bottle's neck [23]. Chen *et al.* [24] studied the properties of auxetic tubular structures which showed decent performance for impact, bending loads, synclastic and conformability around curved objects. Ren *et al.* [25] designed and developed auxetic nails which are easy to penetrate and hard to remove.

The recent progress in design, modelling, and manufacturing has enabled the creation of new auxetic structures for different modern applications. With the help of advanced CAD software, various types of cellular structures can be modelled with different Poisson's ratios from negative to positive. Auxetics are designed in various shapes or geometries in order to obtain desired NPR value in conjunction with other mechanical properties like stiffness, elasticity and modulus of resilience to name a few [26], [26]. The design of auxetics is achieved by defining a geometry through mathematical formulation and design variables and evaluating the effect of these on the mechanical properties like elastic modulus E , bulk modulus K and shear modulus G [27]. Auxetics are also designed by using topology optimisation techniques as discussed by several researchers [28], [29], [30], [31].

Auxetic geometries are modelled and fabricated in two general configurations, 2D thin sheet auxetics [32], [33], [34] and 3D auxetic lattice structures, [29], [35]. Elipe *et al.*, [36] presented a comprehensive study of 2D and 3D auxetic structures and compared the auxetic properties of different designs. Auxetic structures can be designed to exhibit either isotropic or anisotropic properties. For example, an isotropic

auxetic design shows a NPR behaviour that equally expands the metamaterial in two lateral directions (x-axis and y-axis equal) when a tensile force is applied along the z-axis and vice versa [37]. In contrast, anisotropic auxetics behave differently when the load is applied in different orientations. Research in isotropic auxetic structures has shown the importance of different designs and their associated applications in 2D [38] and 3D [29]. With respect to functionality and applications, anisotropic auxetic metamaterials can also be designed to obtain desired mechanical responses, for instance, 2D anisotropic auxetics were used in mechanical actuators and soft robotics [39]. Similarly, 3D anisotropic auxetics are discussed and presented in different research [40].

In recent literature, there has been a growing interest in the design and fabrication of tuneable auxetic metamaterials to achieve a range of desirable mechanical properties such as impact resistance and conformability around complex shapes. 2D auxetic metamaterials have been designed by researchers in different shapes and types such as strut-based structures, extruded patterns, topology-optimized cells, cutting shapes of slits, triangular cuts, chiral, honeycomb and re-entrant [41]. Depending upon the building material and geometrical complexity of the design, a suitable manufacturing process is employed for the fabrication of the auxetic structure. For instance, AM processes such as fused deposition modelling (FDM) [26] and stereolithography (SLA) are commonly used for the fabrication of strut-based and extruded-based auxetic designs. CNC laser-cutting has been utilized for the fabrication of designs which involved slits and cutting geometries [42].

2D auxetic metamaterials have gained significant interest in the mechanical metamaterial design research community. Saeed R. *et al.* [33] developed 2D auxetic metamaterials with hyper-elastic properties using a density-based topology optimisation technique. They observed the deformation mechanism and characteristics of the auxetic metamaterial that were highly dependent upon the topology optimisation variables. Wang *et al.* [34] designed and developed a thin metamaterial film with excellent conformability and adhesion for bandage substrates in order to achieve a non-uniform Poisson's ratio that mimics a functionality similar to human skin.

In several engineering applications, filtration is a common approach for separating particles into different size classes for further physical, chemical, or biological analysis. Conventional filters are designed to capture particles within a specific size range. Developing a smart filtering medium that can effectively work for particles of varying sizes, is a challenging task for the industry. Grima *et al.* [43] are one of the earliest researchers who discussed the potential use of 2D auxetics as a filtering medium. Because the auxetic metamaterial's property depends upon the construction of its unit cell geometry, by scaling the unit cell up and down between the centimetre and nanometre range, the associated filtering property can be scaled proportionally. Mizzi *et al.* [44] studied a nanoscale 2D in-plane auxetic metamaterial and established a relationship eq. (1) to demonstrate how the porosity and aperture shape of the auxetic metamaterial change proportionally upon the applied strain (Figure 2). The aperture size of the metamaterial is controlled by its geometrical design variables and an applied strain as presented in eq. (1).

$$d_s = \sqrt{\left(\frac{p_1}{\frac{p_2}{p_1 - w} + \frac{p_1 - w}{p_2}}\right)^2 + \left[\left(\frac{p_1}{\frac{p_2}{p_1 - w} + \frac{p_1 - w}{p_2}}\right) \frac{p_2}{p_1 - w}\right]^2} \quad \text{eq. (1)}$$

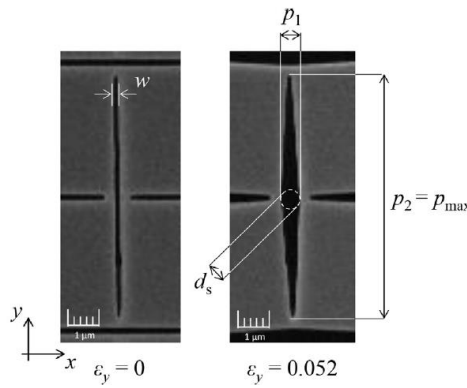


Figure 2 Demonstration of the auxetic cell proposed for particle filtering by Mizzi et al [44]

In eq. (1), d_s represents the size of the passable spherical body, p_1 is the pore parameter, w is the initial width of the slit, and p_2 or p_{max} is the length of the maximum rhombic pore dimension. Their results showed that the porosity was doubled by applying up to 5% strain, allowing a significant increase in the maximum permissible size of the particles passing through the filter.

The potential applications of programmable filtering media can be found in various industrial settings where precise particle separation and filtration is needed. This can involve water filtration, air filtration, chemical and gas filtration, biomedical applications, and the processing of food and beverages. The use of 2D auxetic materials as a filtering medium has not yet been fully investigated in the research community. In this study, the applicability of a 2D auxetic metamaterial for the construction of a smart filtering device is investigated. In contrast to the previous research [44] which only studied the feasibility of such an application, this study presents a novel design of a 2D auxetic structure with a comprehensive solution as a filtering device followed by prototype construction and experimentation. Since the geometrical features of the auxetic cellular structure play an important role in the functionality of the structure as a filtering medium, an optimization approach based on Genetic Algorithm (GA) is proposed and utilised in this study to enable finding the best design for filtration and classification of desired-sized particles. The design is tuned to enable controlled filtration of different-sized particles through an applied strain within a linear elastic region.

2. Methodology

The applied methodology is presented through the following four sections:

- The design strategy for the proposed auxetic filter
- The optimization of the design through a genetic algorithm (GA)
- The finite element analysis (FEA) of the designed auxetic filter
- Additive manufacturing (AM) and mechanical assembly

2.1. The design strategy for the proposed auxetic filter

The novel design of the 2D auxetic unit cell is developed with the help of a set of mathematical equations. This mathematical model is based on parametric equations of torus geometry which were initially developed in Desmos as demonstrated in Figure 3 (a). The corresponding CAD model was then developed in Matlab® as shown in Figure 3 (b).

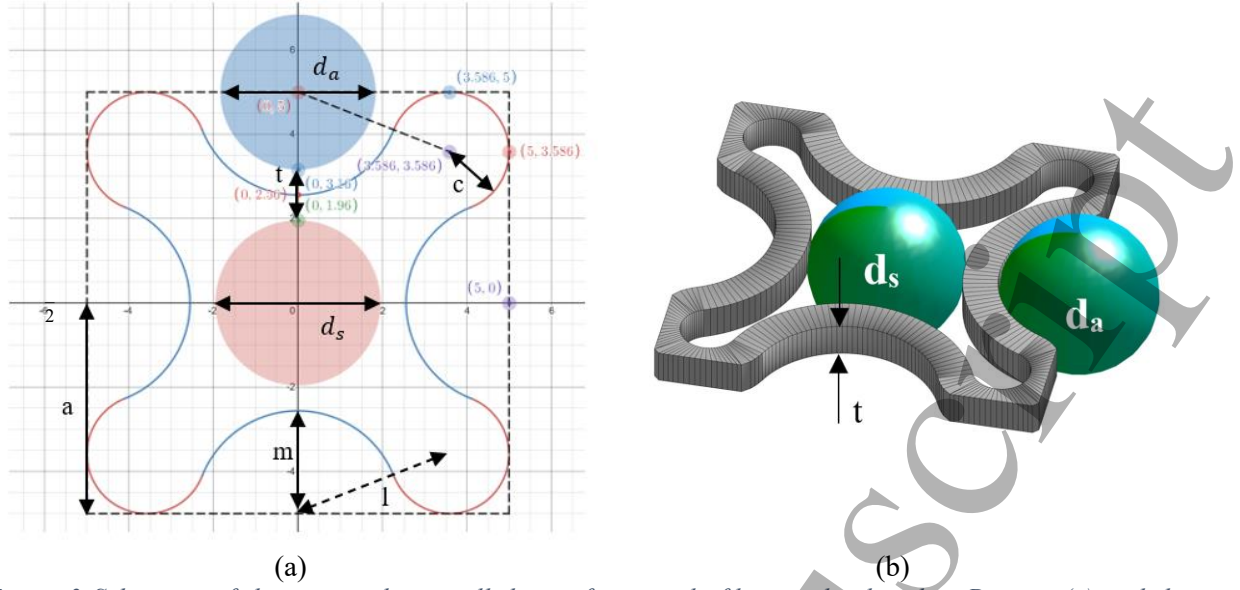


Figure 3 Schematic of the proposed unit cell design for particle filtering developed in Desmos (a) and the corresponding 3D CAD model developed in Matlab (b)

Eqs (2-4) present the relationship between the different geometric design variables as shown in Figure 3 (a):

$$m = \left(\sqrt{\left(\frac{a}{2} - c\right)^2 + \left(\ell - \left(\frac{a}{2} - c\right)\right)^2} \right) - c \quad \text{eq. (2)}$$

$$p = \left(\tan^{-1} \left(\frac{\ell - (a - c)}{\frac{a}{2} - c} \right) \right) \quad \text{eq. (3)}$$

$$d_s = 2 \times (\ell - m - t) \quad \text{eq. (4)}$$

where d_s is the size of the aperture at the cell centre and d_a is the size of the aperture on the edges of the cell, as demonstrated in Figure 3. t represents the strut width/thickness, c is the radius of corner arcs, ℓ is the centre-to-centre distance from corner arc c to edge arc m , p is the constant for the parametric arc, and m represents the radius of the edge arcs. In order to achieve a valid geometry, c/a can vary from 0.12 to 0.19, and ℓ/a can vary from 0.45 to 0.7. The cell centre aperture size to cell size ratio d_s/a varies from 0.27 up to 0.69 and the edge centre aperture size to cell size ratio d_a/a varies from 0.11 to 0.46. d_s is the main aperture calculated from the eq. (4) and the selection of c and ℓ is only valid for the values which will result in $d_s \geq d_a$. These parameter domains were calculated from the given equations eq. (2), eq. (3) and eq. (4) under no load condition that means no strain was applied to the filtering medium. These are presented in dimensionless format since the relationship between the geometrical design variables and particle filtering is scalable.

2.2. The optimization of the design through genetic algorithm (GA)

A Genetic algorithm (GA) developed in Matlab® is utilized to find the best geometry parameters for filtering the desired particle size. GA algorithm mimics the natural selection and evolutionary process to improve certain features following a number of generations [47]. GA has been utilised in structural

optimization and design for AM in previous research [45]. To perform GA in this study, the number of generations was set to 50, population size was set to 20, the number of pairs of chromosomes to cross over in each generation was four and the number of chromosomes to be mutated in each generation was four. A population of potential designs were initially generated based on random allocation of c and ℓ (the two design variables) values within the valid range defined in section 2.1. Each design was represented by a chromosome of 40 bits in length, with 20 bits allocated for each design variable, providing an accuracy of up to five decimal points. The design chromosomes cross over and mutate during each evolutionary iteration to generate new design possibilities. The fittest designs which will proceed to the next generation will be those with lowest values of objective (cost) function. The objective function $f(c, \ell)$ is defined as the difference between the aperture size of the filtering medium and the size of the particle to be filtered, i.e. the optimization program seeks to minimize the gap between the particle and the boundary of the aperture:

$$\text{minimize } f(c, \ell) = |d_s - d_p|/a \quad \text{eq. (5)}$$

where d_p denotes the particle size. The objective function is evaluated in each evolutionary iteration for the whole population of designs to find the best values of design variables c and ℓ and the corresponding geometry. Convergence is achieved when the generation of new designs does not result in a geometry different to the previous generation.

A sample run of the GA program with the above GA parameters was tested to optimise an auxetic structure of cell size 10mm for filtration of particles of size 4mm, i.e. the particle size to cell size ratio (d_p/a) of 0.4. Figure 4 Error! Reference source not found. presents the evolution history and convergence of the objective function. It can be seen that the first generation of potential designs had an average objective of about 0.075 (corresponding to an average size difference of 0.75mm between the particle and the aperture), while the best design in that generation had an objective of nearly 0.025 (corresponding to 0.25mm size difference between the particle and the aperture). Both the average objective and the best objective decreased through the iterative evolutionary optimization process and converged to zero within 40 generations.

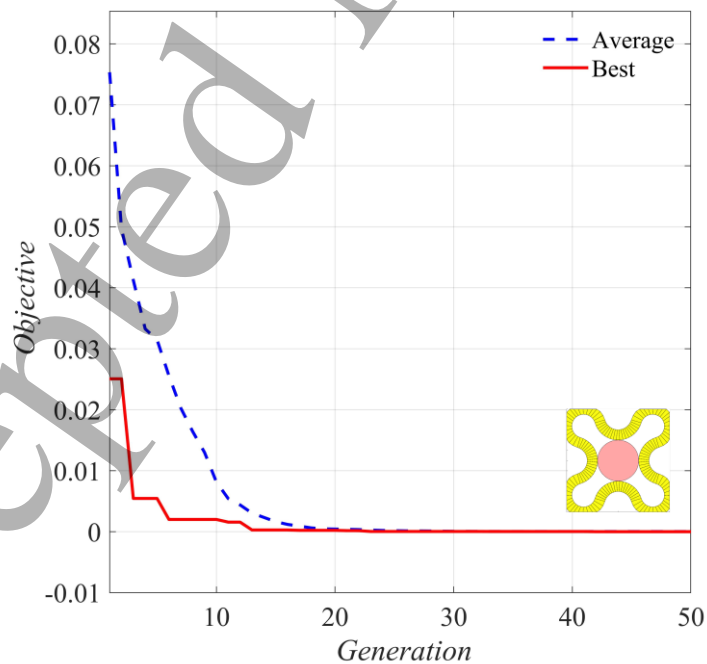


Figure 4 Evolution history of objective (cost) function

2.3. Finite element analysis of the designed auxetic filter

The proposed filtering medium is capable of controlled filtration of particles of different sizes when the medium is under mechanical strain. To calculate the relationship between the aperture size and the strain, a finite element (FE) model of the 2D auxetic structure is developed with the help of the PDE (Partial Differential Equation) toolbox in Matlab®. In the corresponding FE model, boundary conditions of fixed support on one end and deformation on the other end were applied. A tetrahedral mesh was used to generate the FE model of the structure as shown in Figure 5. The max element size of the mesh was $t/4$ and the min element size of the mesh was $t/8$, where t is the strut width as demonstrated in Figure 3.

To investigate the dependency of the results on the utilised FE mesh, a mesh sensitivity analysis was performed as shown in Figure 6. For simplicity, a structure of a 3×3 unit cell array was used. The aperture sizes d_s and d_a were measured and plotted against element size when the structure was under 5% linear strain. As shown in Figure 6, the mesh size does not have a considerable effect on the measured values of aperture sizes d_s and d_a . The verification of FE model through experimentation is presented in section 2.4.

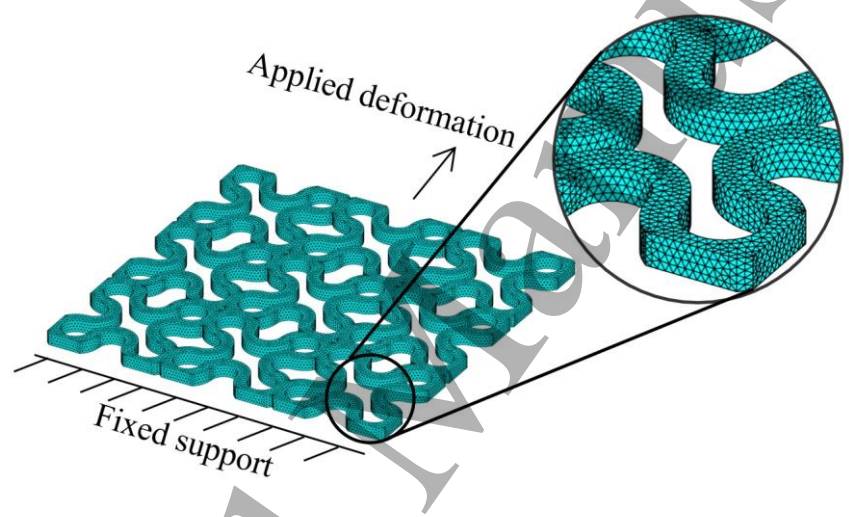


Figure 5 Demonstration of the mesh used for the FE model of filtering medium with a min element size of $t/8$ and max element size of $t/4$.

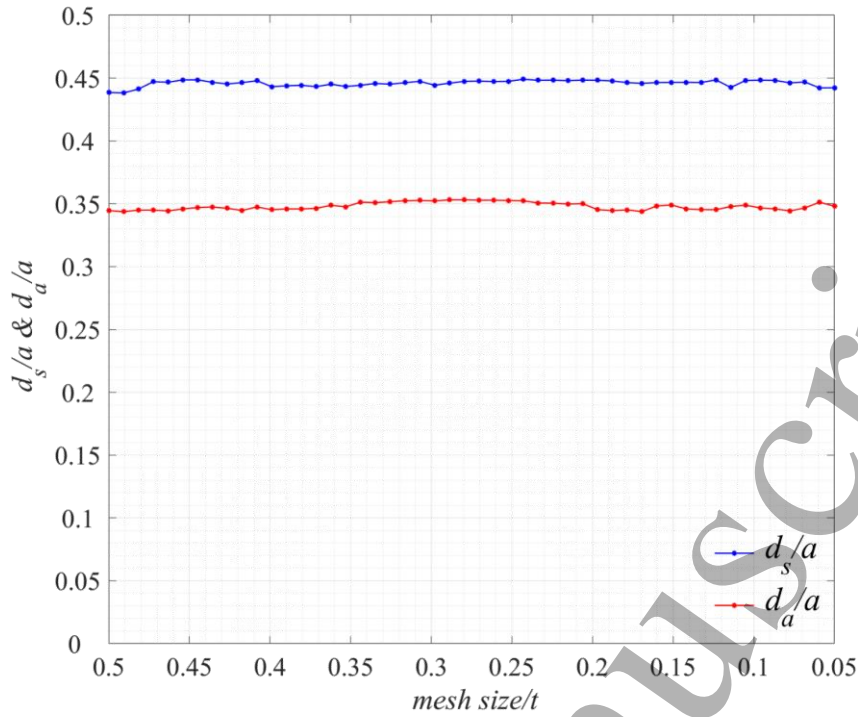


Figure 6 Mesh sensitivity analysis investigating the effect of mesh size on measured values of aperture sizes d_s and d_a when the filtering medium is under 5% strain.

To study the effect of applied strain on the variation of aperture size, the design was initially optimised through the approach presented in Section 2.2 for the filtration of particles of size $d_p > 0.40a$. In this case, the optimised design parameters were obtained as $c = 0.119a$ and $l = 0.543a$. Figure 7 presents the relationship between d_s , d_a and the applied strain. The results show that by increasing the applied strain, the cell centre aperture size d_s increases linearly. Conversely, increasing the applied strain results in reduction of the edge centre aperture size d_a . This is due to the curved shape of the auxetic cell struts shown in Figure 3 (b). When the auxetic structure is stretched under applied tensile strain, the curved strut members tend to become straight. As the cell centre apertures are located on the convex side of the curved struts and the edge centre apertures on the concave side, stretching the auxetic structure results in increasing d_s and reducing d_a . The proposed auxetic filter is designed primarily to deform under tensile strain however, numerical results corresponding to the compression of the filter is also provided in Figure 7 for observation of the behaviour of the filter under compressive strain.

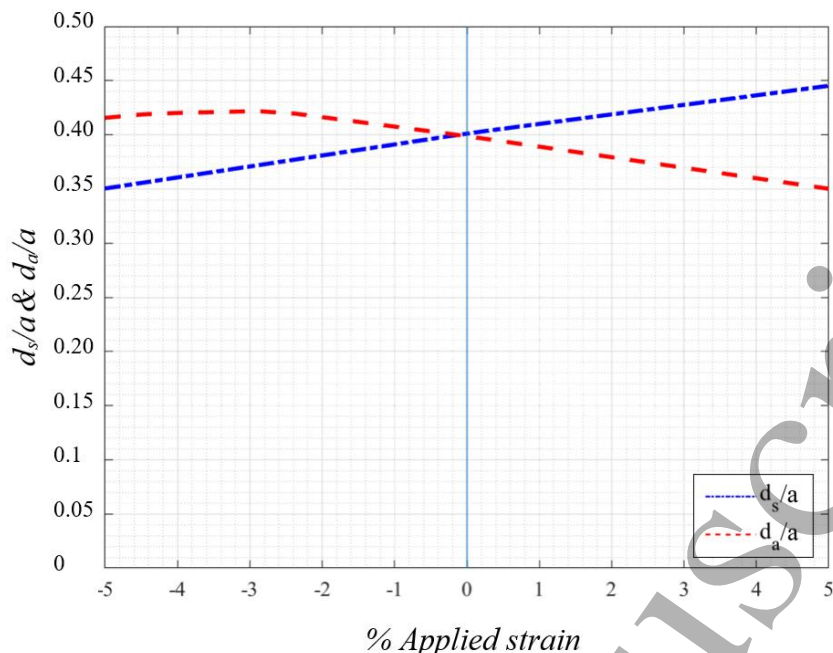


Figure 7 The change in aperture sizes (d_s/a and d_a/a) under the applied linear strain

Figure 8 shows the transverse (x-axis) displacement contour corresponding to the FE model presented in Figure 5, when one end of the structure is fixed and the other end is subjected to an applied displacement of $0.15a$, equivalent to longitudinal strain of $\epsilon_y = 5\%$. This resulted in lateral expansion of $0.012a$ on each side of the structure, equivalent to a transverse strain of $\epsilon_x = 0.8\%$. The Poisson's ratio for the auxetic structure is calculated as $\nu = -\frac{0.8\%}{5\%} = -0.16$.

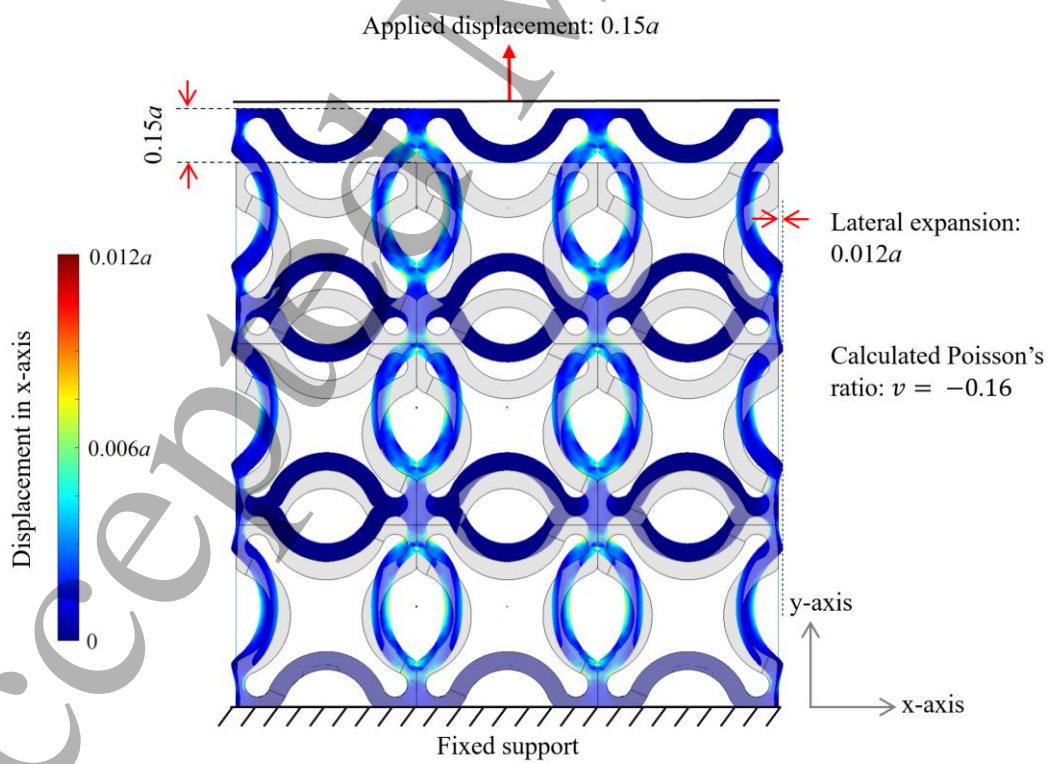


Figure 8 Transverse(x-axis) displacement contour for the auxetic structure under displacement loading.

2.4. Prototyping by using fused deposition modelling (FDM)

The program developed in this study constructs a parametric model of the 2D auxetic structure, optimizes the geometry with respect to desired and then exports that optimized geometry into STL file format which can further be used for the fabrication of the filter through an AM process. A prototype model of the proposed filtering medium was 3D printed through fused deposition modelling (FDM) process using Prusa i3 MK3 machine (Figure 9). The design parameters and global dimensions of the prototype are presented in Table 1. The device consists of a frame, a slider and the proposed 2D auxetic structure which is constructed from 11×7 auxetic unit cells printed from Flexfill TPU 98A [46] with mechanical properties presented in Table 2. The frame and the slider are printed from standard PLA material [47]. 0.4mm nozzle and standard 3D printer settings were used for the fabrication of this prototype.

Table 1 Dimensions and design parameters of the prototyped auxetic filter

Parameter name	symbol	
global length	L	110 mm
global width	W	70 mm
cell size	a	10 mm
strut thickness	t	1 mm
design variable-1	c	1.19 mm
design variable-2	ℓ	5.43 mm
aperture-1 diameter	d_s	4.0 mm
aperture -2 diameter	d_a	4.0 mm

Table 2 Mechanical properties of Flexfill TPU 98A used for fabrication of the auxetic filter [46]

Parameter	Value	Test method	Test condition
Material density	1.23 g/cm ³	ISO 1183-1	
Tensile strength	53.7 MPa	DIN53504	at the break, 200 mm/min
Tensile stress	12.1 MPa	DIN53504	10% elongation 200 mm/min
	22.1 MPa		50% elongation 200 mm/min
	28.4 MPa		100% elongation 200 mm/min
	37.8 MPa		300% elongation 200 mm/min
Elongation at break	318%	DIN53504	200 mm/min
Hardness	98 Shore A	ISO 7619-1	
	60 Shore D		
Tear strength	170 kN/m	ISO 34-1	500 mm/min
Abrasion	23 mm ³	ISO 4649	Method A

The slider can move inside the frame to apply deformation to one end of the auxetic filter while the other end is secured to the frame. The two sides of the filter which are alongside the length of the frame can move freely within the provisions provided in the frame. A small millimetre ruler is printed on the frame to check the applied displacement through the slider. As presented in section 2.3, the proposed

filtering medium has a Poisson's ratio of $\nu = -0.16$ at the current optimized configuration. A small (close to zero) value of Poisson's ratio is advantageous for such application to minimize the lateral deformation of the medium when subjected to deformation, preventing friction, buckling, and out-of-plane deformations. Investigation of these effects is not within the scope of this study.

The feasibility of the proposed device was investigated by distributing different-sized particles (bearing balls of size 4 mm and 4.5 mm), larger than the unstretched filter apertures, on top of the filter and applying a tensile strain by gradually moving the slider. It was observed that by increasing the tensile strain, the aperture size of the filtering medium increased allowing the balls to pass through the filter, thus providing a proof of concept for the proposed programmable particle filtering medium.

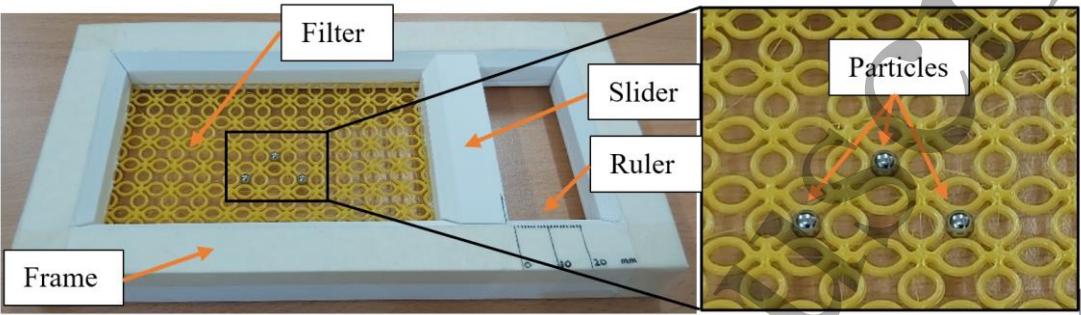


Figure 9 The assembled prototype of the proposed programmable filtering medium

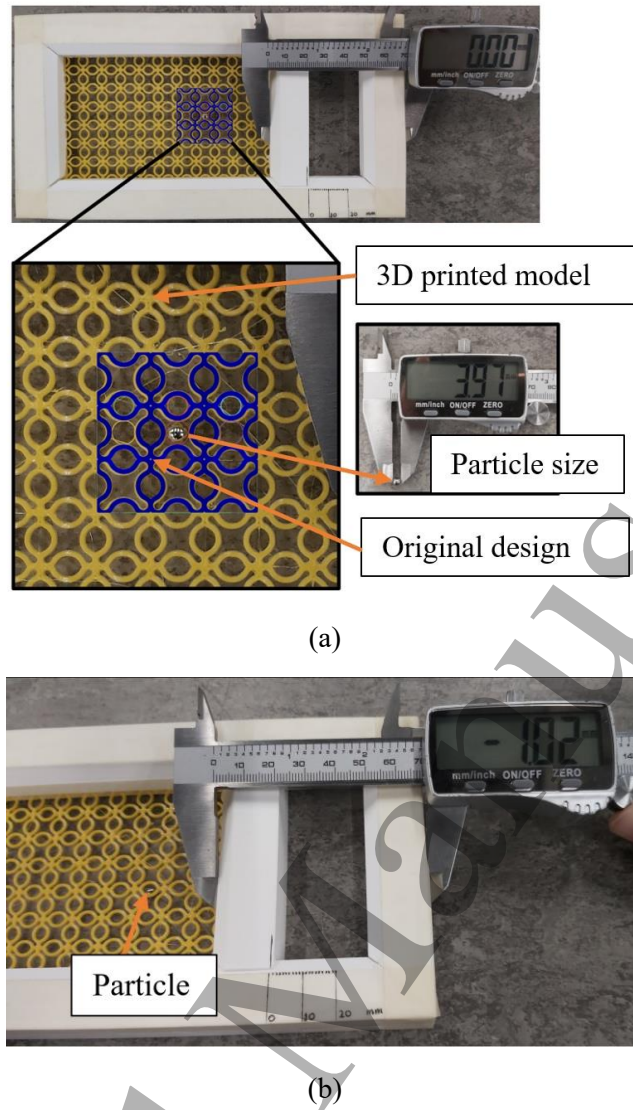


Figure 10 (a) Demonstration of unstretched filter and comparison between the original design (presented in blue colour) and the 3D printed model (presented in yellow colour), (b) measuring the displacement required to allow particles to pass through the filter.

Table 3 Comparison of the applied strain required for passing two different sized particles through the filter and the corresponding filter aperture size calculated through FEA.

	Case-1: 4 mm bearing ball	Case-2: 4.5 mm bearing ball
Exact particle size measured by caliper	3.97 mm	4.49 mm
Minimum applied displacement to let the particle pass through the filter	1.02 mm	6.48 mm
Applied strain corresponding to the above displacement	0.9%	5.9%
Aperture size-unstretched filter	4 mm	4 mm
Aperture size- stretched filter under the applied strain (calculated using FEA)	4.06 mm	4.51 mm

In order to confirm the correlation between the strain applied and the size of the filter aperture, an experiment was conducted where a caliper was attached to the slider to measure the minimum displacement required for each particle to pass through the filter. The corresponding applied strains were calculated from the slider displacement. The aperture size of the stretched filter corresponding to the applied strain was calculated through FEA (see Figure 7) and compared with the size of the particle which passed through. The experiment procedure is demonstrated in Figure 10 and the results are presented in Table 3. Figure 10 (a) shows the unstretched filter with the apertures designed to be 4mm in size. However, it can be seen that the 4 mm bearing ball (3.97 mm measured by caliper) is unable to pass through the unstretched filter. This can be attributed to design-to-build discrepancies of 3D printed parts, which is demonstrated in the figure in blue and yellow colours. In this case, the 3D printed filter was slightly tapered from the base layer and up to the top layer. Additionally, the designed filter apertures need to have some clearance in order for the particles of the same size to pass through. As can be seen from Table 3, when the applied strain increased to 0.9%, the 4mm ball could pass through the filter aperture. At this level of strain, the aperture size is estimated to be 4.06 mm through the FEA. When the experiment was repeated for the 4.5 mm bearing ball, the applied strain increased to 5.9% to enable the particle to pass through the filter. The FEA approximates the aperture size at this strain level to be 4.51 mm which is very close to the particle size 4.49 mm. Overall, the results from this observation suggest that the experimental and FEA measurements corresponding to filter aperture size and applied strain are comparable and the relation can be calibrated by addressing the 3D printing resolution and accuracy.

3. Summary and conclusion:

To summarize this research, a programmable filtering medium was designed for the first time based on the concept of auxetic metamaterials. In the first stage of the design process, the parametric model of a novel auxetic unit cell was developed and its design parameters corresponding to the filtration of a specific particle size were optimised through GA. It was observed that for the proposed unit cell design, the achievable aperture size ranges from 10% to 50% of the cell size. In the second stage, the relation between the applied linear elastic strain and the aperture size of the filtering medium was established with the help of FE simulations. FE simulations showed that a particle filtration range for this particular design configuration allows up to a further 12% variation in the aperture size by applying 5% linear elastic strain. Lastly, a 3D-printed prototype of the proposed filtering medium was developed with the help of the FDM process demonstrating the proof of concept when the prototype was used for the filtration of different-sized particles (bearing balls).

This research stands on the assumption of the linear response of the proposed auxetic metamaterial. Geometric non-linearities response in large deformation and comprehensive experimental validation and calibration is beyond the scope of this research and will be addressed in the forthcoming research work. An important characteristic of the proposed design is scalability which makes the system capable of particle filtering from nano-scale to micro-scale and macro-scale. These properties make this system a potential candidate for implementation as a reconfigurable filtration device in a wide range of applications.

Funding

This study was funded by the Faculty of Computing, Engineering and Media at De Montfort University.

Statements and Declarations

On behalf of all authors, the corresponding author states that there is no conflict of interest.

References

- [1] M. Askari, D. A. Hutchins, P. J. Thomas, L. Astolfi, R. L. Watson, M. Abdi, M. Ricci, S. Laureti, L. Nie and S. Freear, "Additive manufacturing of metamaterials: A review," *Additive manufacturing*, pp. 101562, 2020.
- [2] N. I. Zheludev, "The road ahead for metamaterials," *Science*, vol 328, no 5978, pp. 582-583, 2010.
- [3] H.M.A. Ali, M. Abdi and Y Sun, "Insight into the mechanical properties of 3D printed strut-based lattice structures," *Progress in additive manufacturing*, .
- [4] C. M. Soukoulis and M. Wegener, "Past achievements and future challenges in the development of three-dimensional photonic metamaterials," *Nature photonics*, vol 5, no 9, pp. 523-530, 2011.
- [5] T. Bückmann, M. Thiel, M. Kadic, R. Schittny and M. Wegener, "An elasto-mechanical unfeelability cloak made of pentamode metamaterials," *Nature communications*, vol 5, no 1, pp. 1-6, 2014.
- [6] V.N. Beschastnova and O.I. Taranenko, , "Physical properties of metamaterials," In *Технические и естественные науки*, 2020, pp. 33-37.
- [7] V. M. Shalaev, W. Cai, U. K. Chettiar, H. Yuan, A. K. Sarychev, V. P. Drachev and A. V. Kildishev, "Negative index of refraction in optical metamaterials," *Optics letters*, vol 30, no 24, pp. 3356-3358, 2005.
- [8] K. E. Evans and A. Alderson, "Auxetic materials: Functional materials and structures from lateral thinking!" *Advanced materials*, vol 12, no 9, pp. 617-628, 2000.
- [9] A. Alomarah, S. H. Masood and D. Ruan, "Metamaterials with enhanced mechanical properties and tuneable poisson's ratio," *Smart materials and structures*, vol 31, no 2, pp. 025026, 2022.
- [10] L. Mizzi, E. M. Mahdi, K. Titov, R. Gatt, D. Attard, K. E. Evans, J. N. Grima and J. Tan, "Mechanical metamaterials with star-shaped pores exhibiting negative and zero poisson's ratio," *Materials & design*, vol 146, pp. 28-37, 2018.
- [11] R. Hamzehei, A. Serjouei, N. Wu, A. Zolfagharian and M. Bodaghi, "4D metamaterials with zero poisson's ratio, shape recovery, and energy absorption features," *Advanced engineering materials*, vol 24, no 9, pp. 2200656, 2022.
- [12] R. Hamzehei, A. Zolfagharian, S. Dariushi and M. Bodaghi, "3D-printed bio-inspired zero poisson's ratio graded metamaterials with high energy absorption performance," *Smart materials and structures*, vol 31, no 3, pp. 035001, 2022.
- [13] X. Yu, J. Zhou, H. Liang, Z. Jiang and L. Wu, "Mechanical metamaterials associated with stiffness, rigidity and compressibility: A brief review," *Progress in materials science*, vol 94, pp. 114-173, 2018.

- [14] G. Pacchioni, "Mechanical metamaterials: The strength awakens," *Nature reviews materials*, vol 1, no 3, pp. 1, 2016.
- [15] R. Hamzehei, M. Bodaghi, J. A. I. Martinez, Q. Ji, U. Gwenn, M. Kadic, C. Wang, A. Zolfagharian and N. Wu, "Parrot Beak-Inspired metamaterials with friction and interlocking mechanisms 3D/4D printed in micro and macro scales for supreme energy absorption/dissipation," *Advanced engineering materials*, .
- [16] F. Scarpa, "Auxetic materials for bioprotheses [in the spotlight]," *IEEE signal processing magazine*, vol 25, no 5, pp. 128-126, 2008.
- [17] P. Mardling, A. Alderson, N. Jordan-Mahy and C. L. Le Maitre, "The use of auxetic materials in tissue engineering," *Biomaterials science*, vol 8, no 8, pp. 2074-2083, 2020.
- [18] O. Duncan, T. Shepherd, C. Moroney, L. Foster, P. D. Venkatraman, K. Winwood, T. Allen and A. Alderson, "Review of auxetic materials for sports applications: Expanding options in comfort and protection," *Applied sciences*, vol 8, no 6, pp. 941, 2018.
- [19] Z. Wang and H. Hu, "Auxetic materials and their potential applications in textiles," *Textile research journal*, vol 84, no 15, pp. 1600-1611, 2014.
- [20] W. Wu, X. Song, J. Liang, R. Xia, G. Qian and D. Fang, "Mechanical properties of anti-tetrachiral auxetic stents," *Composite structures*, vol 185, pp. 381-392, 2018.
- [21] A. Zolfagharian, M. Bodaghi, R. Hamzehei, L. Parr, M. Fard and B. F. Rolfe, "3D-printed programmable mechanical metamaterials for vibration isolation and buckling control," *Sustainability*, vol 14, no 11, pp. 6831, 2022.
- [22] R. Brighenti and F. Tatar, "Thermo-mechanical performance of two-dimensional porous metamaterial plates," *International journal of mechanical sciences*, vol 238, pp. 107854, 2023.
- [23] S. P. Silva, M. A. Sabino, E. M. Fernandes, V. M. Correlo, L. F. Boesel and R. L. Reis, "Cork: Properties, capabilities and applications," *International materials reviews*, vol 50, no 6, pp. 345-365, 2005.
- [24] C. Luo, C. Z. Han, X. Y. Zhang, X. G. Zhang, X. Ren and Y. M. Xie, "Design, manufacturing and applications of auxetic tubular structures: A review," *Thin-walled structures*, vol 163, pp. 107682, 2021.
- [25] X. Ren, J. Shen, P. Tran, T. D. Ngo and Y. M. Xie, "Auxetic nail: Design and experimental study," *Composite structures*, vol 184, pp. 288-298, 2018.
- [26] X. Ren, R. Das, P. Tran, T. D. Ngo and Y. M. Xie, "Auxetic metamaterials and structures: A review," *Smart materials and structures*, vol 27, no 2, pp. 023001, 2018.
- [27] Y. Prawoto, "Seeing auxetic materials from the mechanics point of view: A structural review on the negative poisson's ratio," *Computational materials science*, vol 58, pp. 140-153, 2012.
- [28] X. Ren, J. Shen, P. Tran, T. D. Ngo and Y. M. Xie, "Auxetic nail: Design and experimental study," *Composite structures*, vol 184, pp. 288-298, 2018.

- [29] F. Wang, "Systematic design of 3D auxetic lattice materials with programmable poisson's ratio for finite strains," *Journal of the mechanics and physics of solids*, vol 114, pp. 303-318, 2018.
- [30] J. Liu, A. T. Gaynor, S. Chen, Z. Kang, K. Suresh, A. Takezawa, L. Li, J. Kato, J. Tang and C. C. Wang, "Current and future trends in topology optimization for additive manufacturing," *Structural and multidisciplinary optimization*, vol 57, no 6, pp. 2457-2483, 2018.
- [31] J. Gao, H. Xue, L. Gao and Z. Luo, "Topology optimization for auxetic metamaterials based on isogeometric analysis," *Computer methods in applied mechanics and engineering*, vol 352, pp. 211-236, 2019.
- [32] M. Borovinšek, N. Novak, M. Vesenjak, Z. Ren and M. Ulbin, "Designing 2D auxetic structures using multi-objective topology optimization," *Materials science and engineering: A*, vol 795, pp. 139914, 2020.
- [33] S. Rezaei, J. Kadkhodapour, R. Hamzehei, B. Taherkhani, A. P. Anaraki and S. Dariushi, "Design and modeling of the 2D auxetic metamaterials with hyperelastic properties using topology optimization approach," *Photonics and nanostructures-fundamentals and applications*, vol 43, pp. 100868, 2021.
- [34] H. Wang, C. Pan, H. Zhao, T. Wang and Y. Han, "Design of a metamaterial film with excellent conformability and adhesion for bandage substrates," *Journal of the mechanical behavior of biomedical materials*, vol 124, pp. 104799, 2021.
- [35] Y. Xue, P. Gao, L. Zhou and F. Han, "An enhanced three-dimensional auxetic lattice structure with improved property," *Materials*, vol 13, no 4, pp. 1008, 2020.
- [36] J. C. Á Elipse and A. D. Lantada, "Comparative study of auxetic geometries by means of computer-aided design and engineering," *Smart materials and structures*, vol 21, no 10, pp. 105004, 2012.
- [37] S. Czarnecki and P. Wawruch, "The emergence of auxetic material as a result of optimal isotropic design," *Physica status solidi (b)*, vol 252, no 7, pp. 1620-1630, 2015.
- [38] S. Shan, S. H. Kang, Z. Zhao, L. Fang and K. Bertoldi, "Design of planar isotropic negative poisson's ratio structures," *Extreme mechanics letters*, vol 4, pp. 96-102, 2015.
- [39] T. Lim, "An anisotropic auxetic 2D metamaterial based on sliding microstructural mechanism," *Materials*, vol 12, no 3, pp. 429, 2019.
- [40] L. Yang, O. Harrysson, H. West and D. Cormier, "Mechanical properties of 3D re-entrant honeycomb auxetic structures realized via additive manufacturing," *International journal of solids and structures*, vol 69, pp. 475-490, 2015.
- [41] X. Ren, R. Das, P. Tran, T. D. Ngo and Y. M. Xie, "Auxetic metamaterials and structures: A review," *Smart materials and structures*, vol 27, no 2, pp. 023001, 2018.
- [42] Z. Wang, C. Luan, G. Liao, J. Liu, X. Yao and J. Fu, "Progress in auxetic mechanical metamaterials: Structures, characteristics, manufacturing methods, and applications," *Advanced engineering materials*, vol 22, no 10, pp. 2000312, 2020.
- [43] J. N. Grima, "Auxetic metamaterials," *Strasbourg, france*, 2010.

1
2
3
4
5
6
7
8
9
10
11
12
13
14
15
16
17
18
19
20
21
22
23
24
25
26
27
28
29
30
31
32
33
34
35
36
37
38
39
40
41
42
43
44
45
46
47
48
49
50
51
52
53
54
55
56
57
58
59
60

[44] L. Mizzi, E. Salvati, A. Spaggiari, J. Tan and A. M. Korsunsky, "2D auxetic metamaterials with tuneable micro-/nanoscale apertures," *Applied materials today*, vol 20, pp. 100780, 2020.

[45] Y. He, M. Abdi, G. F. Trindade, B. Begines, J. Dubern, E. Prina, A. L. Hook, G. Y. Choong, J. Ledesma and C. J. Tuck, "Exploiting generative design for 3D printing of bacterial biofilm resistant composite devices," *Advanced science*, vol 8, no 15, pp. 2100249, 2021.

[46] fillamentum, "Flexfill TPU 98A technical datasheet," fillamentum, Jan. 2023.

[47] RS Pro, "RS PRO 1.75mm white PLA 3D printer filament, 1kg," RS pro, Jan. 2023.